

Crosstalk Cancellation between Multiple Transmission Lines Based on the Inverse Matrix of Transfer Function Matrix

Yafei Wang^{1,2,*}, Xiaozhe Wang^{1,2}, and Xuehua Li^{1,2}

¹Key Laboratory of Information and Communication Systems, Ministry of Information Industry
Beijing Information Science and Technology University, Beijing 102206, China

²Key Laboratory of Modern Measurement & Control Technology, Ministry of Education
Beijing Information Science and Technology University, Beijing 102206, China

ABSTRACT: Aiming at the crosstalk problem between multiple coupled transmission lines in high-speed interconnection, a crosstalk cancellation method based on the inverse matrix of the Coupled Transmission Lines-Transfer Function Matrix (CTL-TFM) is proposed. The method first constructs the transfer function matrix of multiple coupled microstrip lines, and then designs the corresponding circuit for the inverse matrix of the transfer function matrix at the output ports. This ensures that the transfer function matrix of the entire system is reduced to a unit matrix, effectively reducing the crosstalk between transmission lines. Simulation results show that the quality of the signal eye diagrams at the outputs of all three coupled microstrip lines is significantly improved after using this method, and the crosstalk amplitude and jitter are substantially reduced.

1. INTRODUCTION

With the rapid development of the internet and information technology, integrated circuit technology has continuously advanced, and electronic devices are evolving toward lower power consumption, higher speeds, and miniaturization [1]. As the distances between traces on circuit boards become shorter and the rise times of digital signals become faster, the interference between traces is becoming more severe. To meet the market demand for high-performance electronic products and solve the crosstalk problem, ensuring that signals are not disturbed during transmission on circuit boards has become a key challenge in integrated circuit design.

Crosstalk is one of the four types of signal integrity issues. In high-speed interconnection systems, transmission lines experience not only electric field coupling but also magnetic field coupling. Under the combined effects of both types of coupling, crosstalk occurs [2]. Microstrip lines, due to their simple manufacturing process, cost-effectiveness, and ability to seamlessly integrate with other planar circuits, are widely used in wireless and microwave circuits, including filters, resonators, and phase shifters for various microwave integrated circuits [3]. Furthermore, microstrip lines have excellent impedance control capabilities and faster transmission speeds but are highly susceptible to crosstalk. In recent years, researchers have tried various approaches to reduce crosstalk. Changing the routing structure of microstrip lines can reduce crosstalk, designing patterns such as serpentine or spiral routing, but these methods are limited by layout space [4–7]. Circuit boards can also be analyzed in terms of changing the board material to reduce crosstalk by covering the microstrip lines with a specific material. However,

the use of additional overlay materials and processes increases the cost and can be more complex to manufacture [8, 9]. A crosstalk cancellation circuit is designed at the output of the microstrip line, but its overall effectiveness is limited when being used for crosstalk cancellation between more transmission lines [10]. In [11–13], crosstalk cancellation problem has been explored from the point of view of coding or channel compensation. These methods effectively reduce crosstalk but require introducing circuits at both ends of the system, increasing its complexity.

In addition, crosstalk cancellation can be approached from the perspective of signal processing. By modeling the channels of coupled transmission lines and then processing the channel transfer matrix, crosstalk cancellation can be achieved. Ref. [14] processes the channel transfer matrix of coupled transmission lines using eigenvalue decomposition, constructing a crosstalk cancellation circuit using two unitary matrices and a diagonal matrix, effectively achieving crosstalk cancellation for multiple microstrip transmission lines. However, this method requires circuit construction at both the input and output ends of the transmission lines, which increases complexity. Ref. [15] constructs a channel transfer matrix model for coupled microstrip lines and directly solves the inverse matrix of this matrix. It only requires signal processing at the output, achieving crosstalk cancellation, but this study was limited to modeling and simulation of two coupled microstrip lines. As the number of transmission lines increases, using the inverse matrix of the channel transfer matrix for crosstalk cancellation becomes more challenging, because the elements in the channel transfer matrix inverse matrix are frequency-dependent, complicating the solution process and making circuit implementation difficult.

* Corresponding author: Yafei Wang (wangyafei@bistu.edu.cn).

This paper addresses the crosstalk problem between multiple coupled microstrip lines. Based on the channel transfer matrix, the Coupled Transmission Lines Transfer Function Matrix (CTL-TFM) is optimized and constructed. The inverse matrix of the transfer function matrix for three coupled transmission lines is then solved. Based on the mathematical expression of the inverse matrix, a corresponding circuit is designed. The simulation results demonstrate that the proposed method can effectively reduce both crosstalk amplitude and jitter among three coupled microstrip lines. This work successfully extends the inverse CTL-TFM-based crosstalk cancellation approach from two-line to three-line systems, thereby completing the theoretical framework for crosstalk cancellation. The results not only provide new validation for the universality of this methodology but also establish essential technical verification for its further extension to systems with more transmission lines.

2. THEORETICAL ANALYSIS OF CROSSTALK CANCELLATION

As shown in Figure 1, for parallel coupled microstrip transmission lines, when high-speed signals are transmitted, the coupling between transmission lines can be viewed as a distributed parameter network composed of many small inductors and capacitors. When a signal changes on the attacking line, the voltage change across the mutual capacitance causes a current to flow through it, generating voltage noise on the victim line. This is capacitive coupling; when current flows through the attacking line, it generates a changing magnetic field around it, inducing voltage noise on the victim line through mutual inductance. The combination of capacitive and inductive coupling results in crosstalk.

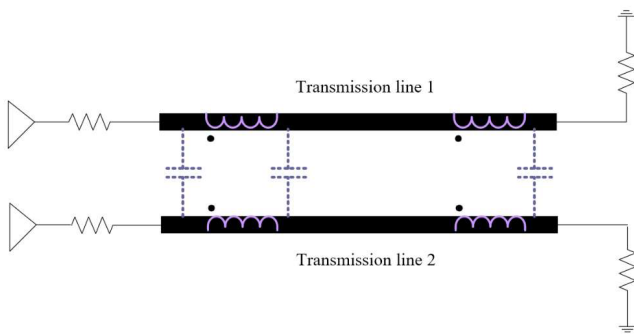


FIGURE 1. Circuit model of two parallel coupled lossless transmission lines.

Based on the theory of crosstalk, for the three parallel coupled microstrip lines shown in Figure 2, the corresponding transfer function matrix can be constructed. In the three coupled microstrip lines, when an excitation signal is input at port 1, due to electromagnetic coupling between transmission lines, far-end crosstalk will occur at ports 5 and 6. When the excitation signal is input at port 2, far-end crosstalk will occur at ports 4 and 6. When the excitation signal is input at port 3, far-end crosstalk will occur at ports 4 and 5. Therefore, the corresponding transfer function matrix model for the three coupled microstrip lines can be established as shown in Figure 3.

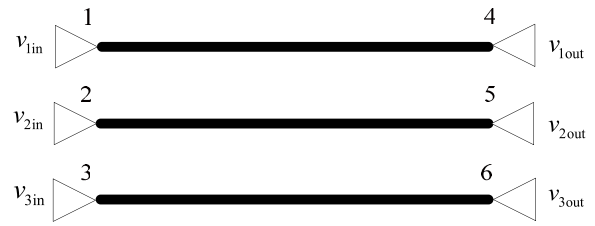


FIGURE 2. Model of three parallel coupled microstrip lines.

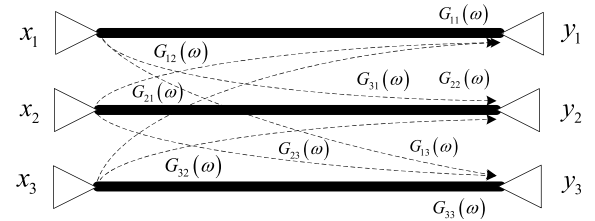


FIGURE 3. Transfer function matrix model for three parallel coupled microstrip lines.

The signal on the transmission line is transmitted in the same direction, with the input signal represented in the frequency domain, denoted as $\mathbf{x} = (x_1, x_2, x_3)^T$; the output signal is denoted as $\mathbf{y} = (y_1, y_2, y_3)^T$; and the transfer function between the j th output port and the i th input port is denoted as $G_{ij}(\omega)$ ($1 \leq i \leq 3, 1 \leq j \leq 3$) $\neq 0$. Due to the electromagnetic coupling between transmission lines, which causes crosstalk, this can be written in matrix form as Equation (1), defining it as CTL-TFM.

$$\mathbf{G}(\omega) = \begin{pmatrix} G_{11}(\omega) & G_{12}(\omega) & G_{13}(\omega) \\ G_{21}(\omega) & G_{22}(\omega) & G_{23}(\omega) \\ G_{31}(\omega) & G_{32}(\omega) & G_{33}(\omega) \end{pmatrix} \quad (1)$$

Thus, the output-input relationship of the signal on the coupled microstrip lines can be expressed as:

$$\mathbf{y} = \mathbf{G}(\omega) \mathbf{x} \quad (2)$$

Clearly, the crosstalk information is concentrated in the transfer function matrix, and how to process this matrix determines the effectiveness of crosstalk cancellation. Since 75% of crosstalk in coupled microstrip lines originates from adjacent lines when the line width equals the line spacing, Equation (1) can be simplified by considering only the crosstalk between adjacent lines. The simplified transfer function matrix is given by:

$$\mathbf{G}(\omega) = \begin{pmatrix} G_{11}(\omega) & G_{12}(\omega) & 0 \\ G_{21}(\omega) & G_{22}(\omega) & G_{23}(\omega) \\ 0 & G_{32}(\omega) & G_{33}(\omega) \end{pmatrix} \quad (3)$$

From the reciprocity of crosstalk: $G_{ij}(\omega) = G_{ji}(\omega)$ ($1 \leq i \leq 3, 1 \leq j \leq 3, i \neq j$), and considering that the parameters of the transmission lines are approximately the same, Equation (3) can be further simplified to:

$$\mathbf{G}(\omega) = \begin{pmatrix} g(\omega) & c(\omega) & 0 \\ c(\omega) & g(\omega) & c(\omega) \\ 0 & c(\omega) & g(\omega) \end{pmatrix} \quad (4)$$

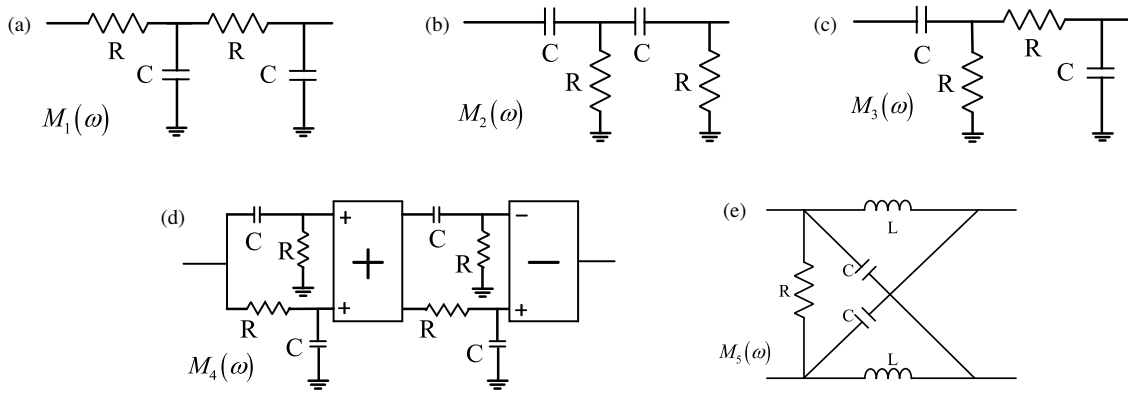


FIGURE 4. Circuit design corresponding to the inverse matrix elements of CTL-TFM. (a) The circuit design corresponding to $M_1(\omega)$. (b) The circuit design corresponding to $M_2(\omega)$. (c) The circuit design corresponding to $M_3(\omega)$. (d) The circuit design corresponding to $M_4(\omega)$. (e) The circuit design corresponding to $M_5(\omega)$.

where $g(\omega)$ represents the transfer function on an individual microstrip line, and $c(\omega)$ is the far-end crosstalk transfer function between adjacent microstrip lines. Further, since $c(\omega) = -j\omega\tau g(\omega)$ [τ is the crosstalk coupling coefficient], Equation (4) becomes:

$$\mathbf{G}(\omega) = g(\omega) \begin{pmatrix} 1 & -j\omega\tau & 0 \\ -j\omega\tau & 1 & -j\omega\tau \\ 0 & -j\omega\tau & 1 \end{pmatrix} \quad (5)$$

Let $\mathbf{G}(\omega) = g(\omega)\mathbf{M}(\omega)$. Theoretically, if matrix $\mathbf{M}(\omega)$ is a unit matrix, the crosstalk between the coupled microstrip lines will be eliminated. The most direct way to achieve this is to multiply its inverse matrix, $\mathbf{M}(\omega)\mathbf{M}(\omega)^{-1} = \mathbf{I}$. Based on this idea, the solution can be expressed as Equation (6):

$$\mathbf{M}(\omega)^{-1} = \frac{1}{1 + 2\omega^2\tau^2} \begin{pmatrix} 1 + \omega^2\tau^2 & j\omega\tau & -\omega^2\tau^2 \\ j\omega\tau & 1 & j\omega\tau \\ -\omega^2\tau^2 & j\omega\tau & 1 + \omega^2\tau^2 \end{pmatrix} \quad (6)$$

By constructing the corresponding circuit at the output of the three microstrip lines according to the form of Equation (6), the input signal passes through the three coupled transmission lines and then through the inverse matrix circuit. This enables crosstalk-free transmission or minimization of crosstalk at the output.

3. CIRCUIT DESIGN FOR THE INVERSE MATRIX OF THE TRANSFER FUNCTION MATRIX

Based on the formulation of Equation (6), this section develops the corresponding circuit implementation. Accounting for design realizability and complexity constraints, we decompose Equation (6) mathematically, leading to the realizable form presented in Equation (7).

$$\mathbf{M}(\omega)^{-1} = \frac{1}{(1 + \sqrt{2}j\omega\tau)^2} \begin{pmatrix} 1 + \omega^2\tau^2 & j\omega\tau & -\omega^2\tau^2 \\ j\omega\tau & 1 & j\omega\tau \\ -\omega^2\tau^2 & j\omega\tau & 1 + \omega^2\tau^2 \end{pmatrix}$$

$$\frac{1 + \sqrt{2}j\omega\tau}{1 - \sqrt{2}j\omega\tau} \quad (7)$$

In Equation (7), the term $1 + \sqrt{2}j\omega\tau/1 - \sqrt{2}j\omega\tau$ corresponding to each element is designed separately, denoted as $M_5(\omega)$. The inverse matrix consists of four types of elements $M_1(\omega)$, $M_2(\omega)$, $M_3(\omega)$, $M_4(\omega)$, each of which needs to be designed into its corresponding circuit. For convenience, each element is further decomposed, as shown in Equations (8)–(11):

$$M_1(\omega) = \frac{1}{(1 + \sqrt{2}j\omega\tau)^2} = \frac{1}{1 + \sqrt{2}j\omega\tau} \times \frac{1}{1 + \sqrt{2}j\omega\tau} \quad (8)$$

$$M_2(\omega) = \frac{-\omega^2\tau^2}{(1 + \sqrt{2}j\omega\tau)^2} = \frac{j\omega\tau}{1 + \sqrt{2}j\omega\tau} \times \frac{j\omega\tau}{1 + \sqrt{2}j\omega\tau} \quad (9)$$

$$M_3(\omega) = \frac{j\omega\tau}{(1 + \sqrt{2}j\omega\tau)^2} = \frac{j\omega\tau}{1 + \sqrt{2}j\omega\tau} \times \frac{1}{1 + \sqrt{2}j\omega\tau} \quad (10)$$

$$M_4(\omega) = \frac{1 + \omega^2\tau^2}{(1 + \sqrt{2}j\omega\tau)^2} = \left(\frac{1}{1 + \sqrt{2}j\omega\tau} + \frac{j\omega\tau}{1 + \sqrt{2}j\omega\tau} \right) \times \left(\frac{1}{1 + \sqrt{2}j\omega\tau} - \frac{j\omega\tau}{1 + \sqrt{2}j\omega\tau} \right) \quad (11)$$

where $1/1 + \sqrt{2}j\omega\tau$ can be implemented using a first-order RC integrator circuit. Therefore, two first-order RC integrator circuits are used for $M_1(\omega)$; $j\omega\tau/1 + \sqrt{2}j\omega\tau$ can be implemented using a first-order RC differentiator circuit, so two first-order RC differentiator circuits are used for $M_2(\omega)$. Similarly, $M_3(\omega)$ is implemented for the first-order RC integral circuit and first-order RC differential circuit. Specifically, four first-order RC circuits are used for $M_4(\omega)$. The specific circuit designs for each element are shown in Figures 4(a), 4(b), 4(c), and 4(d). The circuit design equivalent to $1 + \sqrt{2}j\omega\tau/1 - \sqrt{2}j\omega\tau$ in Equation (7) is shown in Figure 4(e), where the specific values of R , C , L are determined according to the value of τ .

Thus, according to Equations (5) and (7), it can be known that the total system transfer function matrix composed of three

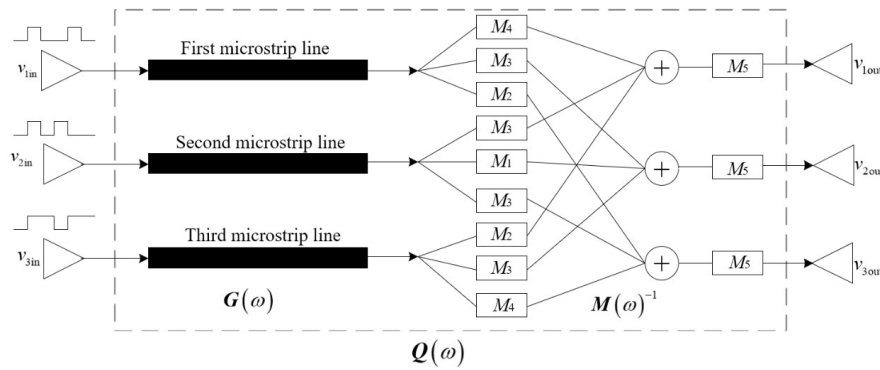


FIGURE 5. Crosstalk cancellation method based on the inverse matrix of CTL-TFM.

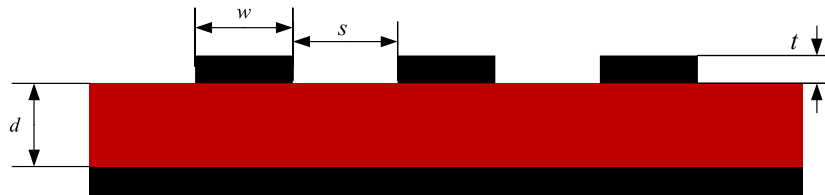


FIGURE 6. Side view of three parallel coupled microstrip line structures.

coupled microstrip lines and the inverse matrix circuit is:

$$\mathbf{Q}(\omega) = \mathbf{G}(\omega) \mathbf{M}(\omega)^{-1} = \frac{g(\omega)}{(1 + \sqrt{2j\omega\tau})^2}$$

$$\begin{pmatrix} 1 & -j\omega\tau & 0 \\ -j\omega\tau & 1 & -j\omega\tau \\ 0 & -j\omega\tau & 1 \end{pmatrix} \begin{pmatrix} 1 + \omega^2\tau^2 & j\omega\tau & -\omega^2\tau^2 \\ j\omega\tau & 1 & j\omega\tau \\ -\omega^2\tau^2 & j\omega\tau & 1 + \omega^2\tau^2 \end{pmatrix}$$

$$\frac{1 + \sqrt{2j\omega\tau}}{1 - \sqrt{2j\omega\tau}} = g(\omega) \begin{pmatrix} 1 & 0 & 0 \\ 0 & 1 & 0 \\ 0 & 0 & 1 \end{pmatrix} \quad (12)$$

Equation (12) indicates that if the inverse matrix circuit is placed at the output end of the coupled transmission line, then the total system transfer function matrix achieves the predetermined goal: $\mathbf{Q}(\omega) = g(\omega)\mathbf{I}$. Theoretically, crosstalk cancellation is realized.

According to Equation (12), the crosstalk cancellation scheme among three transmission lines based on the inverse matrix of the transfer function matrix of the coupled transmission line is constructed as shown in Figure 5. The circuit modules M_1, M_2, M_3, M_4, M_5 correspond to the circuits in Figure 4, namely $M_1(\omega), M_2(\omega), M_3(\omega), M_4(\omega), M_5(\omega)$.

4. SIMULATION AND RESULT ANALYSIS

In this section, advanced design system software (ADS) is used to simulate and verify the effectiveness of the proposed method. The TLines-Microstrip module in ADS is used to create three parallel microstrip transmission lines. As shown in Figure 6,

the microstrip line has a width of 1 mm, a thickness of 70 μm , a line spacing of 1 mm, a length of 10 cm, and a dielectric board thickness of 0.56 mm, with a relative permittivity $\epsilon_r = 4.6$, $\mu_r = 1$. According to Figure 5, the CTL-TFM inverse matrix circuit is constructed at the output ports of the coupled transmission lines, with the values of R, C, L in the circuit are determined by synthesizing them based on the value of τ . The circuit is impedance-matched to 50 Ω at each port.

A pseudo-random sequence with a rate of 5 Gbit/s and a length of $2^{15}-1$ is fed into the input of three coupled microstrip transmission lines. The amplitude of the signal is 1 V; the rise (fall) time is 20 ps; and the signal numbers are synchronized. The quality of the signals at the outputs on the transmission lines before and after using the proposed method is simulated. The eye diagram of the signal at the output end can intuitively reflect the jitter in time and the crosstalk in amplitude of the signal, the simulation results of the eye diagram are shown in Figure 7. After using the proposed method, the original closed eye diagram opens up; the shape of the eye diagram is more regular and clearer; the noise tolerance of the eye diagram is significantly improved; and the jitter and distortion of the signal are effectively improved, which verifies the effectiveness of the method.

In order to further verify the effectiveness of the proposed method, the signal of the second transmission line (the intermediate transmission line) is delayed by half a codeword, while the signals of the other two lines are kept at normal input, so as to verify the effectiveness of the proposed method under the non-synchronized signal. The other parameters set in the simulation are the same as above, and the simulation results are shown in Figure 8, which show that the proposed method is still effective

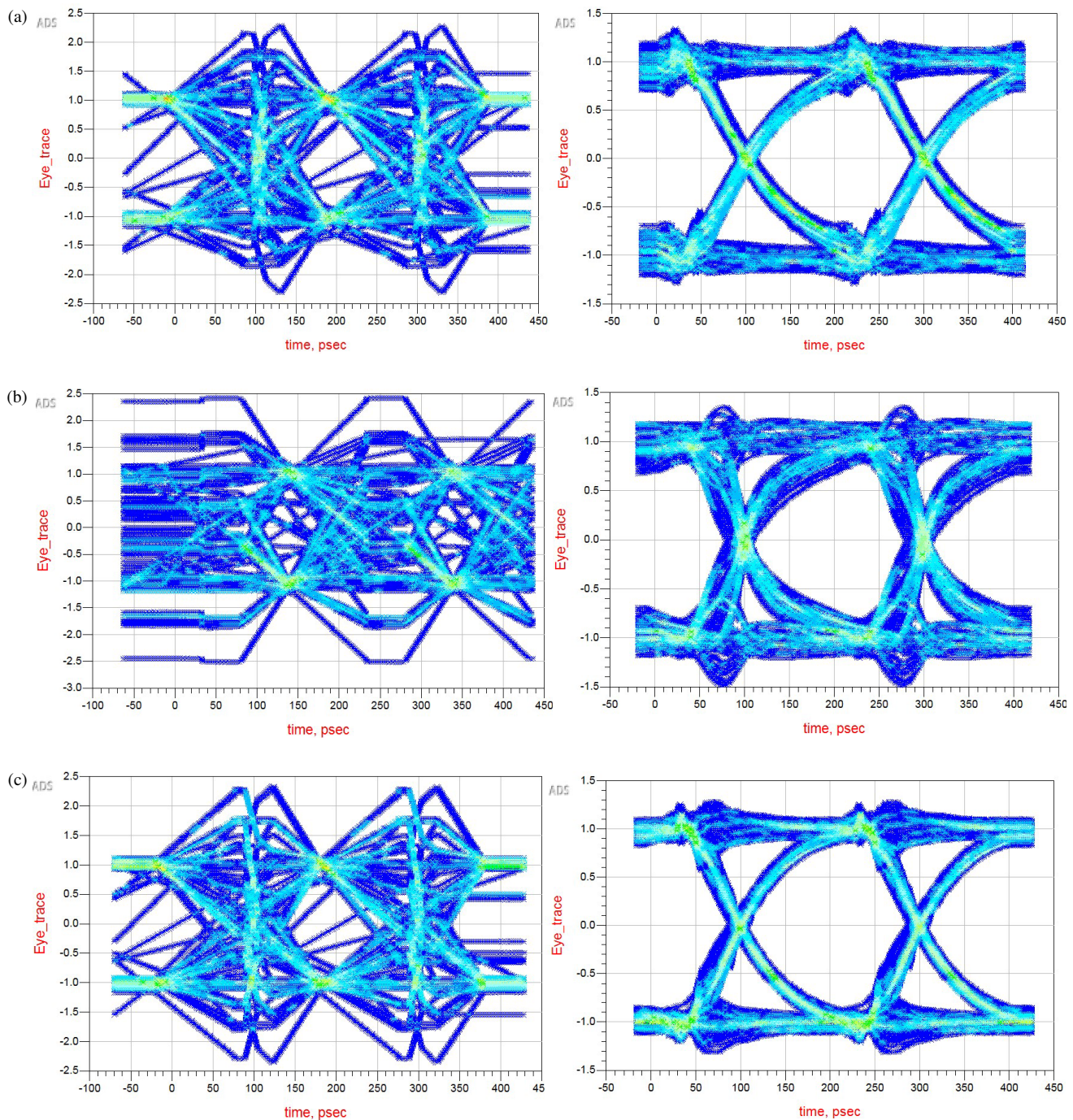


FIGURE 7. Eye diagram comparison before and after crosstalk cancellation when excitation signals are synchronized. (a) First microstrip line comparison. (b) Comparison of the second microstrip line (the middle microstrip line). (c) Third microstrip line comparison.

in suppressing crosstalk, and the crosstalk cancellation effect is good.

The simulation results of the eye diagram show that the proposed crosstalk cancellation method among three transmission lines based on the inverse matrix of the transfer function matrix works well under the input signal rate of 5 Gbit/s. Crosstalk cancellation is achieved by signal processing only once at the output of the transmission line, which reduces the signal processing at the input end of the transmission line, in the case

of not much difference in the effect of the crosstalk cancellation method based on the decomposition of channel transmission matrix. In terms of stability or reliability, the primary processing of the inverse matrix method in this paper is better than the secondary processing of the eigenvalue decomposition method [14]. In addition, simulation has also verified that there is no significant change in the eye diagram when the component values in the inverse matrix circuit deviate within 5%.

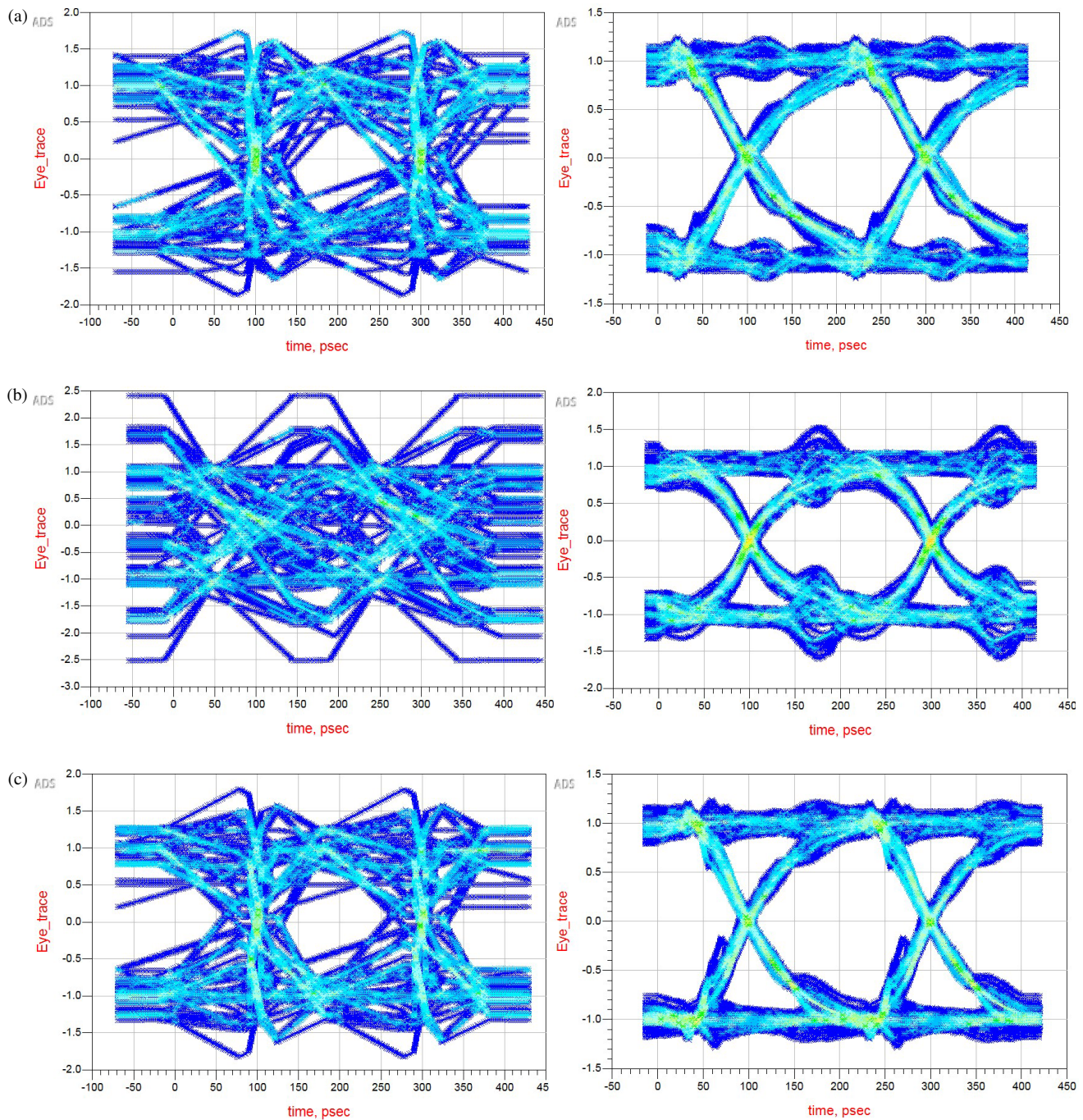


FIGURE 8. Comparison of eye diagrams before and after crosstalk cancellation when the excitation signal is not synchronized. (a) First microstrip line comparison. (b) Comparison of the second microstrip line (the middle microstrip line). (c) Third microstrip line comparison.

5. CONCLUSION

This paper addresses the crosstalk problem between multiple coupled microstrip lines. The transfer function matrix for three coupled microstrip transmission lines is constructed. Based on theoretical analysis, a crosstalk cancellation circuit is designed using the inverse matrix of the coupled transmission line transfer function matrix. By transforming the transfer function matrix of overall system into a unit matrix, crosstalk cancellation is achieved. This method only requires one signal processing step at the output end to achieve crosstalk cancellation. The

effectiveness of the proposed method is verified through ADS simulation. The method is successfully applied to a transition from two transmission lines to three, providing new validation for the universality of the crosstalk cancellation method based on the inverse matrix of the coupled transmission line transfer function matrix.

REFERENCES

- [1] Cai, J.-D., K.-C. Chen, and C.-L. Wang, "Mode conversion and common-mode noise reduction using periodic structure filter,"

- IEEE Transactions on Electromagnetic Compatibility*, Vol. 64, No. 4, 1021–1030, 2022.
- [2] Halligan, M. S. and D. G. Beetner, “Maximum crosstalk estimation in weakly coupled transmission lines,” *IEEE Transactions on Electromagnetic Compatibility*, Vol. 56, No. 3, 736–744, 2014.
- [3] Phromlounsri, R., S. Sonasang, S. Srisawat, T. Cheawchanwatana, N. Panit, and M. Chongcheawchamnan, “Microstrip coupled lines crosstalk reducing using center step impedance transmission lines,” in *2023 7th International Conference on Information Technology (InCIT)*, 364–368, Chiang Rai, Thailand, Nov. 2023.
- [4] Zhechev, Y. S., A. O. Belousov, A. M. Zabolotsky, S. V. Vlasov, M. S. Murmanskyy, N. S. Pavlov, and T. R. Gazizov, “Routing technique for microwave transmission lines to ensure UWB interference immunity,” *IEEE Transactions on Microwave Theory and Techniques*, Vol. 71, No. 12, 5304–5316, 2023.
- [5] Liu, Y., S. Bai, B. Pu, J. Lee, and D. H. Kim, “Analysis on unintentional resonances in high-speed signals from non-ideal routing stub,” in *2021 IEEE International Joint EMC/SI/PI and EMC Europe Symposium*, 994–999, Raleigh, NC, USA, Jul.-Aug. 2021.
- [6] Pandey, G., A. Patel, S. Chandrasekaran, G. Verma, N. S. S. Sankaran, and R. Panigrahi, “Time domain enhancement of tab-routed microstrip line with EMC validation for DDR4 memory design,” in *2023 IEEE Microwaves, Antennas, and Propagation Conference (MAPCON)*, 1–4, Ahmedabad, India, Dec. 2023.
- [7] Ge, J., R. Floyd, A. Khan, and G. Wang, “High-performance interconnects with reduced far-end crosstalk for high-speed ICs and communication systems,” *IEEE Transactions on Components, Packaging and Manufacturing Technology*, Vol. 13, No. 7, 1013–1020, 2023.
- [8] Lin, Z., X. Cao, Q.-M. Cai, Y. Ren, X. Ye, and J. Fan, “Sensitivity analysis of local soldermask and coverlay in high speed transmission lines for DDR5 applications to reduce FEXT,” in *2020 IEEE International Symposium on Electromagnetic Compatibility & Signal/Power Integrity (EMCSI)*, 586–590, Reno, NV, USA, Jul.-Aug. 2020.
- [9] Cai, Q.-M., Y. Zhu, R. Zhang, Y. Ren, X. Ye, and J. Fan, “A study of coverlay coated microstrip lines for crosstalk reduction in DDR5,” in *2020 IEEE International Symposium on Electromagnetic Compatibility & Signal/Power Integrity (EMCSI)*, 581–585, Reno, NV, USA, Jul.-Aug. 2020.
- [10] Jeong, Y.-U., S. Choi, S. Kim, and J.-H. Chae, “Single-ended receiver-side crosstalk cancellation with independent gain and timing control for minimum residual FEXT,” *IEEE Transactions on Circuits and Systems I: Regular Papers*, Vol. 70, No. 12, 4793–4803, 2023.
- [11] Chen, G.-Y. and T.-C. Lee, “An 8 Gb/s far-end crosstalk cancellation and FFE co-designed TX output driver,” *IEEE Solid-State Circuits Letters*, Vol. 7, 227–230, 2024.
- [12] Kim, H., H. Seo, Y. Jo, C. Yoo, and J. Han, “An 8b9b 77.44-Gb/s noise-immune spatial-delta coded transceiver for short-reach memory interfaces in 28-nm CMOS,” *IEEE Transactions on Circuits and Systems II: Express Briefs*, Vol. 70, No. 4, 1301–1305, 2022.
- [13] Liu, Q., L. Du, and Y. Du, “A 0.90-Tb/s/in 1.29-pJ/b wireline transceiver with single-ended crosstalk cancellation coding scheme for high-density interconnects,” *IEEE Journal of Solid-State Circuits*, Vol. 58, No. 8, 2326–2336, 2023.
- [14] Wang, Y. F., Y. X. Zhao, W. Yang, *et al.*, “Modeling of transmission matrix and crosstalk cancellation method and effect analysis of coupled transmission line,” *Acta Electronica Sinica*, Vol. 47, No. 5, 1129–1135, 2019.
- [15] Ding, H. and Y. Wang, “Crosstalk reduction between microstrip lines based on inverse matrix of channel transmission matrix,” *Telecommunication Engineering*, Vol. 58, No. 9, 1086–1090, 2018.
- [16] Oh, T. and R. Harjani, “A 6-Gb/s MIMO crosstalk cancellation scheme for high-speed I/Os,” *IEEE Journal of Solid-State Circuits*, Vol. 46, No. 8, 1843–1856, 2011.